Analysis of the giant spin Hall effect in Cu(Bi) alloys

Dmitry V. Fedorov,* Christian Herschbach, Annika Johansson, Sergey Ostanin, and Ingrid Mertig
Max Planck Institute of Microstructure Physics, Weinberg 2, 06120 Halle, Germany and Institute of Physics, Martin Luther University Halle-Wittenberg, 06099 Halle, Germany

Martin Gradhand
H. H. Wills Physics Laboratory, University of Bristol, Bristol BS8 1TL, United Kingdom

Kristina Chadova, Diemo Ködderitzsch, and Hubert Ebert
Department of Chemistry, Physical Chemistry, Ludwig-Maximilians University, Munich, Germany
(Received 26 March 2013; revised manuscript received 7 August 2013; published 19 August 2013)

Two years after the prediction of a giant spin Hall effect for the dilute Cu(Bi) alloy [Gradhand *et al.*, Phys. Rev. B **81**, 245109 (2010)], a comparably strong effect was measured in thin films of Cu(Bi) alloys by Niimi *et al.* [Phys. Rev. Lett. **109**, 156602 (2012)]. Both theory and experiment consider the skew-scattering mechanism to be responsible, however they obtain opposite sign for the spin Hall angle. Based on a detailed analysis of the obtained theoretical results, we propose that either the formation of extremely small clusters or the influence of interface roughness and grain boundaries decorated with Bi atoms are responsible for the observed phenomenon.

DOI: 10.1103/PhysRevB.88.085116 PACS number(s): 72.25.Ba, 71.15.Rf, 75.76.+j, 85.75.−d

I. INTRODUCTION

One of the most interesting phenomena related to the field of spintronics is the spin Hall effect (SHE).[1,2] It provides the opportunity to create spin currents in nonmagnetic materials avoiding injection from a ferromagnet. For practical applications, materials with a large spin Hall angle (SHA), the efficiency of charge to spin current conversion, are desirable. The first measurement of a giant SHE was reported for Au with a SHA of 0.11.[3] Recently, a giant SHA of −0.12 to −0.15 was measured in highly resistive β-Ta,[4] in accordance with a qualitative prediction based on a tight-binding model for bcc Ta.[5] Comparably large SHA's were predicted for Au(C) (Ref. 6) and for Cu(Bi) (Ref. 7) dilute alloys from first-principles calculations. For thin films of Cu(Bi) alloys the giant SHE was recently confirmed experimentally.[8] However, the sign of the measured spin Hall angle (−0.24) is opposite to the *ab initio* result (0.08), although in both studies skew scattering at substitutional Bi impurities is assumed to be the origin of the considered effect.

In this paper we provide an analysis of theoretical and experimental results and conclude that the sign of the SHE measured in thin-film Cu(Bi) alloys cannot be explained by the conventional skew scattering at substitutional Bi impurities in Cu bulk. Our study is based on first-principles calculations using the semiclassical Boltzmann equation[6] and the quantum-mechanical Kubo-Středa formula.[9] In addition, we present a generalized version of the resonant scattering model used in Ref. 8. We demonstrate that this model applied to the considered phenomenon provides good agreement with the *ab initio* calculations.

To exclude any possible confusions from the outset, first of all we consider the definition of the SHA used in our work and its relation to other approaches.

II. DEFINITION OF THE SPIN HALL ANGLE

The sign of the SHA is a subtle point since different sign conventions for the spin Hall conductivity (SHC) are used in the literature. This complicates a comparison between various approaches. One definition uses the SHC in units of the charge conductivity with the corresponding prefactor of e^2 as in Refs. 6 and 7 as well as in Refs. 10 and 11. Its advantage is the coherent treatment of spin and charge conductivities providing the dimensionless spin Hall angle as their ratio. In addition, for materials like copper with spin expectation values of the Bloch states close to 1 (in units of $\hbar/2$),[12] the two-current model can be employed. Within this model, the charge and spin Hall current densities are given by $j_x = j_x^+ + j_x^- = \sigma_{xx}E_x = (\sigma_{xx}^+ + \sigma_{xx}^-)E_x$ and $j_y^s = j_y^+ - j_y^- = \sigma_{yx}^s E_x = (\sigma_{yx}^+ - \sigma_{yx}^-)E_x$, respectively. Here "+" and "−" denote the two spin channels contributing to the charge conductivity σ_{xx} and the spin Hall conductivity σ_{yx}^s as linear-response functions to an applied electric field $\boldsymbol{E} = (E_x,0,0)$. Although this appears natural within the semiclassical theory,[6,7,10,11] the most common definition is related to the Kubo theory.[13–15] Here, the SHC has the prefactor of $(-e)(\hbar/2)$ replacing the electron charge $(-e)$ by the spin units $\hbar/2$. Such a definition provides opposite sign in comparison to the first one. Finally, one can use the SHC expressed in units of the charge conductivity but keeping the sign from the common definition of the Kubo formula.[13–15] This was done in Ref. 9 exploiting the Kubo-Středa formula.

Throughout this paper the SHC, denoted as σ_{H}^s, will refer to σ_{yx}^s of Refs. 6 and 7, σ_{xy}^s of Ref. 9, and $\frac{2e}{\hbar}\sigma_{xy}^s$ of Refs. 13–15. Taking into account that for the systems with both time and space inversion symmetry the relation $\sigma_{xy}^s = -\sigma_{yx}^s$ is valid, this convention provides a consistent comparison of different approaches. Clearly, the sign of the SHC determines the sign of the spin Hall angle $\alpha = \sigma_{\mathrm{H}}^s/\sigma_{xx}$ used to quantify the SHE. This quantity is perfectly suited for the skew-scattering mechanism where α is independent of the impurity concentration.[6,9]

III. COMPARISON TO EXPERIMENTAL DATA

After these introductory comments, let us compare experimental and theoretical results. A negative value of the SHA was measured for Cu(Bi) alloys, while a positive sign of the SHE

was reported for the Cu(Ir) alloy and for pure Pt (see Fig. 2 of Ref. 8). It is commonly assumed that the SHE in Pt is related to the intrinsic mechanism, since reproducible experimental results are in good agreement with theoretical predictions.[9,16] These *ab initio* calculations confirm in particular the sign of σ_{H}^{s}. Moreover, the extrinsic contribution was shown to be small for this material.[9,17] An agreement between experiment and theory is also obtained for the Cu(Ir) alloy. Considering the skew-scattering mechanism, we obtain $\alpha = 0.035$ and $\alpha = 0.029$ from the Boltzmann equation and the Kubo-Středa formula, respectively, while the experimental value is 0.023.[8] For this alloy, both the charge and spin resistivities show almost perfect linear dependence on the impurity concentration up to 12 at. %.[8,18] This indicates the dominance of the skew-scattering mechanism for the SHE in Cu(Ir). By contrast, for the Cu(Bi) alloy the experimental results deviate from the linear dependence above 0.5 at. % impurity concentration.[8] To handle this problem, lower concentrations were chosen for the measurement. As a result, a negative SHA of -0.24 was measured in contradiction to first-principles calculations.[7] To clarify this issue, we perform a detailed analysis of existing as well as new *ab initio* results in comparison to the experiment. Furthermore, we derive a generalized phase-shift model as an extension of the resonant scattering model of Ref. 8 and simulate the scattering conditions needed to reproduce the experimental data.

IV. GENERALIZED RELATIVISTIC PHASE-SHIFT MODEL FOR THE SPIN HALL EFFECT

The semiclassical approach in spherical band approximation provides the following expression for the conductivity tensor of a crystal:

$$\hat{\sigma} = \frac{e^2}{V}\sum_{\mathbf{k}} \delta(\mathcal{E}_{\mathbf{k}} - \mathcal{E}_F)\mathbf{v}_{\mathbf{k}} \circ \mathbf{\Lambda}_{\mathbf{k}} = \frac{e^2 m_e k_F}{\hbar^2 (2\pi)^3}\int d\Omega_{\mathbf{k}}\, \mathbf{v}_{\mathbf{k}} \circ \mathbf{\Lambda}_{\mathbf{k}}, \tag{1}$$

evaluated with

$$\mathcal{E}_{\mathbf{k}} = \frac{\hbar^2 k^2}{2m_e}, \quad \frac{1}{V}\sum_{\mathbf{k}} \delta(\mathcal{E}_{\mathbf{k}} - \mathcal{E}_F) \to \frac{m_e k_F}{\hbar^2 (2\pi)^3}\int d\Omega_{\mathbf{k}}. \tag{2}$$

Here V is the system volume and $\int d\Omega_{\mathbf{k}}$ refers to an integration over the angular part of the crystal momentum $\mathbf{k}$. The mean free path in Eq. (1) is given by the Boltzmann equation[19]

$$\mathbf{\Lambda}_{\mathbf{k}} = \tau_{\mathbf{k}}(\mathbf{v}_{\mathbf{k}} + \sum_{\mathbf{k}'} P_{\mathbf{k}\leftarrow\mathbf{k}'}\mathbf{\Lambda}_{\mathbf{k}'}), \tag{3}$$

where the momentum relaxation time $\tau_{\mathbf{k}}$ is defined as

$$\frac{1}{\tau_{\mathbf{k}}} = \sum_{\mathbf{k}'} P_{\mathbf{k}'\leftarrow\mathbf{k}} = \frac{2\pi}{\hbar} c_i N \sum_{\mathbf{k}'} |T_{\mathbf{k}'\leftarrow\mathbf{k}}|^2 \delta(\mathcal{E}_{\mathbf{k}} - \mathcal{E}_{\mathbf{k}'}) \tag{4}$$

and $\mathbf{v}_{\mathbf{k}} = \hbar\mathbf{k}/m_e$ is the group velocity. The microscopic transition probability $P_{\mathbf{k}'\leftarrow\mathbf{k}}$ describes the rate of scattering from an initial state $\mathbf{k}$ into a final state $\mathbf{k}'$. This quantity is defined by the corresponding transition matrix $T_{\mathbf{k}'\leftarrow\mathbf{k}}$ and scales with the impurity concentration c_i and the total number of atoms N in the system.[19] This scaling holds for the dilute limit of noninteracting scatterers valid for impurity concentrations less than a few at. %.

TABLE I. The Clebsch-Gordan coefficients from Ref. 20.

j	$m_s = -1/2$	$m_s = 1/2$
$l - 1/2$	$\sqrt{\frac{l+m+1/2}{2l+1}}$	$-\sqrt{\frac{l-m+1/2}{2l+1}}$
$l + 1/2$	$\sqrt{\frac{l-m+1/2}{2l+1}}$	$\sqrt{\frac{l+m+1/2}{2l+1}}$

The derivation presented below is based on a relativistic scattering theory within the spherical band approximation, as considered in Ref. 20. Using Eq. (11.72) of this book, the amplitudes for the spin-conserving and spin-flip scattering of an initial state $\mathbf{k}$, chosen from the relativistic "spin-up" ("+") channel, into a final state $\mathbf{k}'$ can be obtained as[21]

$$f^{+\leftarrow+}_{\mathbf{k}'\leftarrow\mathbf{k}} = \frac{4\pi}{k_F}\sum_j \sum_{m_j=-j}^{+j} C\left(l\tfrac{1}{2}j; m_j - \tfrac{1}{2}, \tfrac{1}{2}\right) e^{i\delta_j}\sin\delta_j \times C\left(l\tfrac{1}{2}j; m_j - \tfrac{1}{2}, \tfrac{1}{2}\right)\left(Y_l^{m_j-1/2}(\hat{\mathbf{k}})\right)^* Y_l^{m_j-1/2}(\hat{\mathbf{k}}') \tag{5}$$

and

$$f^{-\leftarrow+}_{\mathbf{k}'\leftarrow\mathbf{k}} = \frac{4\pi}{k_F}\sum_j \sum_{m_j=-j}^{+j} C\left(l\tfrac{1}{2}j; m_j - \tfrac{1}{2}, \tfrac{1}{2}\right) e^{i\delta_j}\sin\delta_j \times C\left(l\tfrac{1}{2}j; m_j + \tfrac{1}{2}, -\tfrac{1}{2}\right)\left(Y_l^{m_j-1/2}(\hat{\mathbf{k}})\right)^* Y_l^{m_j+1/2}(\hat{\mathbf{k}}'), \tag{6}$$

respectively. Here δ_j is the phase shift related to the relativistic quantum number $j = l \pm 1/2$, which corresponds to the spin-orbit splitting of levels with the orbital quantum number l. The expansion into the spherical harmonics Y_l^m is performed via the Clebsch-Gordan coefficients $C(l\frac{1}{2}j; m - m_s, m_s)$ given by Table I.

The scattering amplitude $f_{\mathbf{k}'\leftarrow\mathbf{k}}$ is related to the corresponding transition matrix[22]

$$T_{\mathbf{k}'\leftarrow\mathbf{k}} = -\frac{2\pi\hbar^2}{m_e V} f_{\mathbf{k}'\leftarrow\mathbf{k}}. \tag{7}$$

Then, for the spin-conserving and spin-flip scattering we obtain

$$T^{+\leftarrow+}_{\mathbf{k}'\leftarrow\mathbf{k}} = -\frac{8\pi^2\hbar^2}{m_e k_F V}\sum_{lm}\left(Y_l^m(\hat{\mathbf{k}})\right)^* Y_l^m(\hat{\mathbf{k}}') \times\left[\left(\frac{l+m+1}{2l+1}\right)e^{i\delta_{l+1/2}}\sin\delta_{l+1/2} + \left(\frac{l-m}{2l+1}\right)e^{i\delta_{l-1/2}}\sin\delta_{l-1/2}\right] \tag{8}$$

and

$$T^{-\leftarrow+}_{\mathbf{k}'\leftarrow\mathbf{k}} = -\frac{8\pi^2\hbar^2}{m_e k_F V}\sum_{lm}\left(Y_l^m(\hat{\mathbf{k}})\right)^* Y_l^{m+1}(\hat{\mathbf{k}}') \times\frac{\sqrt{(l-m)(l+m+1)}}{2l+1} \times[e^{i\delta_{l+1/2}}\sin\delta_{l+1/2} - e^{i\delta_{l-1/2}}\sin\delta_{l-1/2}], \tag{9}$$

respectively.

Following Eqs. (2) and (4), the corresponding relaxation time can be written as

$$\frac{1}{\tau_{\mathbf{k}}^{+}} = \frac{1}{\tau_{\mathbf{k}}^{+\leftarrow+}} + \frac{1}{\tau_{\mathbf{k}}^{-\leftarrow+}} = \frac{c_i N m_e k_F V}{\hbar^3 (2\pi)^2} \int d\Omega_{\mathbf{k}'} (|T_{\mathbf{k}'\leftarrow\mathbf{k}}^{+\leftarrow+}|^2 + |T_{\mathbf{k}'\leftarrow\mathbf{k}}^{-\leftarrow+}|^2). \quad (10)$$

Similar to Ref. 11, we will use the isotropic relaxation time approximation $\tau_{\mathbf{k}} \approx \tau_0 = \text{const}$ further on. Within this approximation, we assume $\tau_0 = \tau_{\mathbf{k}_0}$, where $\mathbf{k}_0 = (0;0;k_F)$. Taking into account that $Y_l^m(\hat{\mathbf{z}}) = \sqrt{\frac{2l+1}{4\pi}}\delta_{m,0}$ and using Eqs. (8) and (9) for the spin-conserving and spin-flip part of the isotropic relaxation time we obtain

$$\frac{1}{\tau_0^{+\leftarrow+}} = \frac{4\pi\hbar c_i}{m_e k_F V_0} \sum_l \left\{ \frac{(l+1)^2}{2l+1} \sin^2\delta_{l+1/2} + \frac{l^2}{2l+1}\sin^2\delta_{l-1/2} + \frac{2l(l+1)}{2l+1}\cos(\delta_{l+1/2}-\delta_{l-1/2}) \times \sin\delta_{l+1/2}\sin\delta_{l-1/2} \right\} \quad (11)$$

and

$$\frac{1}{\tau_0^{-\leftarrow+}} = \frac{4\pi\hbar c_i}{m_e k_F V_0} \sum_l \frac{l(l+1)}{2l+1} \{\sin^2\delta_{l+1/2} + \sin^2\delta_{l-1/2} - 2\cos(\delta_{l+1/2}-\delta_{l-1/2})\sin\delta_{l+1/2}\sin\delta_{l-1/2}\}, \quad (12)$$

respectively. Their sum gives us

$$\frac{1}{\tau_0} = \frac{4\pi\hbar c_i}{m_e k_F V_0} \sum_l [(l+1)\sin^2\delta_{l+1/2} + l\sin^2\delta_{l-1/2}], \quad (13)$$

where $V_0 = V/N$ is the unit-cell volume. Here we have used the relation $\tau_0 = \tau_0^+ = \tau_0^-$, which is valid due to the time inversion symmetry of the considered systems.

Alternatively, one could use the relation between the relaxation time and the scattering cross section $\sigma_{\text{cs}} = V_0/v_F c_i \tau_0$.[23] Together with the well-known expression for the relativistic scattering cross section [see, for instance, Eq. (11.74) of Ref. 20]

$$\sigma_{\text{cs}} = \frac{4\pi}{k_F^2} \sum_l [(l+1)\sin^2\delta_{l+1/2} + l\sin^2\delta_{l-1/2}], \quad (14)$$

this easily provides the expression for the relaxation time given by Eq. (13).

With respect to the Hall conductivity caused by the skew-scattering mechanism, the first term on the right-hand side of Eq. (3) is unimportant since only the *scattering-in* term (vertex corrections) contributes to this quantity.[6,9] Moreover, only the antisymmetric part $P_{\mathbf{k}\leftarrow\mathbf{k}'}^{\text{antisym}} = (P_{\mathbf{k}\leftarrow\mathbf{k}'} - P_{\mathbf{k}'\leftarrow\mathbf{k}})/2$ of the microscopic transition probability provides a nonvanishing contribution.[10,11] In addition, we will use the approximation $\mathbf{\Lambda}_{\mathbf{k}'} \to \tau_{\mathbf{k}'}\mathbf{v}_{\mathbf{k}'}$ for the scattering-in term in Eq. (3), similar to Ref. 11. Then, neglecting spin-flip transitions, the Hall component of the conductivity tensor $\hat{\sigma}^+$ is given by

$$\sigma_{yx}^{+} = \frac{c_i N V e^2 k_F^2 \tau_0^2}{\hbar^3 (2\pi)^5} \int d\Omega_{\mathbf{k}} \int d\Omega_{\mathbf{k}'}\, k_y k_x' |T_{\mathbf{k}\leftarrow\mathbf{k}'}^{+\leftarrow+}|^2_{\text{antisym}} \quad (15)$$

with $|T_{\mathbf{k}\leftarrow\mathbf{k}'}^{+\leftarrow+}|^2_{\text{antisym}} = (|T_{\mathbf{k}\leftarrow\mathbf{k}'}^{+\leftarrow+}|^2 - |T_{\mathbf{k}'\leftarrow\mathbf{k}}^{+\leftarrow+}|^2)/2$.

Let us rewrite Eq. (8) in the following form:

$$T_{\mathbf{k}'\leftarrow\mathbf{k}}^{+\leftarrow+} = -\frac{8\pi^2\hbar^2}{m_e k_F V} \sum_{lm} \frac{(Y_l^m(\hat{\mathbf{k}}))^* Y_l^m(\hat{\mathbf{k}}')}{2l+1} \times \{m[e^{i\delta_{l+1/2}}\sin\delta_{l+1/2} - e^{i\delta_{l-1/2}}\sin\delta_{l-1/2}] + (l+1)e^{i\delta_{l+1/2}}\sin\delta_{l+1/2} + l e^{i\delta_{l-1/2}}\sin\delta_{l-1/2}\}. \quad (16)$$

As was already pointed out in Ref. 11, the term $\sum_m m(Y_l^m(\hat{\mathbf{k}}))^* Y_l^m(\hat{\mathbf{k}}')$ is antisymmetric with respect to exchange of $\mathbf{k}$ and $\mathbf{k}'$, while $\sum_m (Y_l^m(\hat{\mathbf{k}}))^* Y_l^m(\hat{\mathbf{k}}')$ is symmetric. Consequently, one can show that

$$|T_{\mathbf{k}'\leftarrow\mathbf{k}}^{+\leftarrow+}|^2_{\text{antisym}} = (|T_{\mathbf{k}'\leftarrow\mathbf{k}}^{+\leftarrow+}|^2 - |T_{\mathbf{k}\leftarrow\mathbf{k}'}^{+\leftarrow+}|^2)/2 = \frac{128\pi^4\hbar^4}{m_e^2 k_F^2 V^2} i \sum_{lm}\sum_{l'm'} m \frac{Y_l^m(\hat{\mathbf{k}})\left(Y_l^m(\hat{\mathbf{k}}')\right)^*\left(Y_{l'}^{m'}(\hat{\mathbf{k}})\right)^* Y_{l'}^{m'}(\hat{\mathbf{k}}')}{2l+1} f_{ll'}, \quad (17)$$

where

$$f_{ll'} = \{(l'+1)\sin(\delta_{l'+1/2}-\delta_{l+1/2})\sin\delta_{l+1/2}\sin\delta_{l'+1/2} + l'\sin(\delta_{l'-1/2}-\delta_{l+1/2})\sin\delta_{l+1/2}\sin\delta_{l'-1/2} - (l'+1)\sin(\delta_{l'+1/2}-\delta_{l-1/2})\sin\delta_{l-1/2}\sin\delta_{l'+1/2} - l'\sin(\delta_{l'-1/2}-\delta_{l-1/2})\sin\delta_{l-1/2}\sin\delta_{l'-1/2}\}/(2l'+1). \quad (18)$$

To derive the Hall component of the conductivity tensor $\hat{\sigma}^+$, one can interchange $\mathbf{k}$ and $\mathbf{k}'$ in Eq. (15) and use Eq. (17). With this procedure we obtain

$$\sigma_{yx}^{+} = \frac{c_i N V e^2 k_F^2 \tau_0^2}{\hbar^3 (2\pi)^5} \int d\Omega_{\mathbf{k}'} \int d\Omega_{\mathbf{k}}\, k_y' k_x |T_{\mathbf{k}'\leftarrow\mathbf{k}}^{+\leftarrow+}|^2_{\text{antisym}} = \frac{e^2\hbar k_F^2 c_i}{\pi m_e^2 V_0}\tau_0^2 \sum_{lm}\sum_{l'm'} \frac{m f_{ll'}}{2l+1} \left\{ \delta_{l',l+1}\left[\delta_{m',m-1}\frac{(l-m+1)(l-m+2)}{(2l+1)(2l+3)} - \delta_{m',m+1}\frac{(l+m+1)(l+m+2)}{(2l+1)(2l+3)} \right] + \delta_{l',l-1}\left[\delta_{m',m-1}\frac{(l+m)(l+m-1)}{(2l-1)(2l+1)} - \delta_{m',m+1}\frac{(l-m)(l-m-1)}{(2l-1)(2l+1)} \right] \right\}. \quad (19)$$

Here we have used the relations

$$k_x = \frac{k_F\sqrt{2\pi}\left[Y_1^{-1}(\hat{\mathbf{k}}) - Y_1^1(\hat{\mathbf{k}})\right]}{\sqrt{3}},\ k_y' = \frac{i k_F\sqrt{2\pi}\left[Y_1^{-1}(\hat{\mathbf{k}}') + Y_1^1(\hat{\mathbf{k}}')\right]}{\sqrt{3}} \quad (20)$$

together with[24]

$$\int Y_l^m[Y_1^{-1}-Y_1^1](Y_{l'}^{m'})^* d\Omega = -\sqrt{\frac{3}{8\pi}}\left\{\delta_{l',l+1}\left[\delta_{m',m+1}\sqrt{\frac{(l+m+1)(l+m+2)}{(2l+1)(2l+3)}}-\delta_{m',m-1}\sqrt{\frac{(l-m+1)(l-m+2)}{(2l+1)(2l+3)}}\right]\right.$$
$$\left.-\delta_{l',l-1}\left[\delta_{m',m+1}\sqrt{\frac{(l-m)(l-m-1)}{(2l-1)(2l+1)}}-\delta_{m',m-1}\sqrt{\frac{(l+m)(l+m-1)}{(2l-1)(2l+1)}}\right]\right\} \quad (21)$$

and

$$\int Y_{l'}^{m'}[Y_1^{1}+Y_1^{-1}](Y_l^{m})^* d\Omega = -\sqrt{\frac{3}{8\pi}}\left\{\delta_{l',l+1}\left[\delta_{m',m+1}\sqrt{\frac{(l+m+1)(l+m+2)}{(2l+1)(2l+3)}}+\delta_{m',m-1}\sqrt{\frac{(l-m+1)(l-m+2)}{(2l+1)(2l+3)}}\right]\right.$$
$$\left.-\delta_{l',l-1}\left[\delta_{m',m+1}\sqrt{\frac{(l-m)(l-m-1)}{(2l-1)(2l+1)}}+\delta_{m',m-1}\sqrt{\frac{(l+m)(l+m-1)}{(2l-1)(2l+1)}}\right]\right\}. \quad (22)$$

If we restrict our consideration to the contributions of s, p, d, and f electrons and neglect terms with $l > 3$, then Eq. (19) can be reduced to the form

$$\sigma_{yx}^{+} = \frac{4e^2\hbar k_F^2 c_i}{\pi m_e^2 V_0}\tau_0^2\left\{\frac{1}{9}(f_{10}-f_{12})+\frac{1}{5}(f_{21}-f_{23})+\frac{2}{7}f_{32}\right\}, \quad (23)$$

where $f_{10},\ldots,f_{32}$ are defined by Eq. (18).

According to Eqs. (1) and (2), the longitudinal conductivity within the isotropic relaxation time approximation is given by

$$\sigma_{xx}^{+} = \frac{e^2 m_e k_F \tau_0}{\hbar^2(2\pi)^3}\int d\Omega_{\mathbf{k}}\, v_{\mathbf{k}}^x v_{\mathbf{k}}^x = \frac{e^2 k_F \tau_0}{m_e(2\pi)^3}\int d\Omega_{\mathbf{k}}\, k_x^2, \quad (24)$$

neglecting the scattering-in term in Eq. (3). Taking into account Eq. (20), we have

$$\int d\Omega_{\mathbf{k}}\, k_x^2 = \frac{4\pi k_F^2}{3}\int d\Omega_{\mathbf{k}}[Y_1^1(\mathbf{k})]^* Y_1^1(\mathbf{k}) = \frac{4\pi k_F^2}{3}, \quad (25)$$

that together with Eq. (24) provides us the longitudinal conductivity

$$\sigma_{xx}^{+} = \frac{e^2 k_F^3}{6\pi^2 m_e}\tau_0 \quad (26)$$

in terms of the momentum relaxation time given by Eq. (13).

The presence of both time and space inversion symmetry provides the following relations between the two spin channels: $\sigma_{xx}^{+} = \sigma_{xx}^{-}$ and $\sigma_{yx}^{+} = -\sigma_{yx}^{-}$. Thus, within the two-current model discussed in Sec. II, the spin Hall angle can be written as

$$\alpha = (\sigma_{yx}^{+}-\sigma_{yx}^{-})/(\sigma_{xx}^{+}+\sigma_{xx}^{-}) = \sigma_{yx}^{+}/\sigma_{xx}^{+}. \quad (27)$$

For comparison with Eq. (2) of Ref. 8, we skip in Eqs. (13) and (23) all terms with $l > 1$, assuming they are negligible for the scattering at Bi atoms. Then, using Eq. (27), we obtain for the SHA

$$\alpha = \frac{2\sin\delta_{1/2}^s[\sin\delta_{1/2}^p\sin(\delta_{1/2}^p-\delta_{1/2}^s)-\sin\delta_{3/2}^p\sin(\delta_{3/2}^p-\delta_{1/2}^s)]}{3(\sin^2\delta_{1/2}^s+\sin^2\delta_{1/2}^p+2\sin^2\delta_{3/2}^p)}, \quad (28)$$

where $\delta_{1/2}^s$ is the phase shift related to s electrons ($l = 0$), while $\delta_{1/2}^p$ and $\delta_{3/2}^p$ are the phase shifts of p electrons ($l = 1$) split by spin-orbit coupling (SOC). Equation (28) is equivalent to Eq. (2) of Ref. 8 but with opposite sign.

The origin of this discrepancy arises from the scattering-in term of the Boltzmann equation. In our case it is used according to Kohn and Luttinger.[25] By contrast, Eq. (2) of Ref. 8 was based on an erroneous scattering-in term used for the Boltzmann equation that caused opposite sign in the SHA.[26]

V. RESULTS AND DISCUSSION

The phase shifts, used for the calculation of the SHA by Eq. (28), were obtained according to Eq. (11.61) of Ref. 20 by means of the relativistic Korringa-Kohn-Rostoker Green's-function method.[12] Within the parent lattice geometry they are the following: $\delta_{1/2}^s = 0.94$, $\delta_{1/2}^p = 1.32$, and $\delta_{3/2}^p = 0.79$.

Up to now structural relaxation next to the impurity atom was neglected in the first-principles description of the SHE.[6,7,9] In order to clarify the influence of this effect on the considered phenomenon, here we will also present the SHA calculated taking into account both the charge and lattice relaxation around the impurity.

The relaxed geometry for Bi and Ir impurities in a Cu host is presented in Table II. This was obtained by means of Vienna *Ab initio* Simulation Package (VASP).[27] The electron-ion interactions are represented by the projector-augmented wave (PAW) pseudopotential[28] and the electronic wave functions expanded as plane waves with the cutoff energy of 450 eV. The corresponding system was simulated with a 108-atom supercell and the relaxation was performed until the forces were less than 5×10^{-3} eV/Å. The obtained structural relaxation for the Bi impurity is much stronger in comparison to the Ir impurity. Therefore, one could assume that the discrepancy between theory and experiment for the Cu(Bi) alloy, in contrast to a good agreement obtained for the Cu(Ir) alloy, is caused by this effect. To perform the transport calculations for the Cu(Bi) alloy, we neglect the structural relaxation for the next-nearest neighbors and take the averaged (over the row) value of 5.6% for the nearest neighbors. The phase shifts corresponding to

TABLE II. The relative extension (in %) of the distances from Bi and Ir impurities to the nearest neighbors (NN) and the next-nearest neighbors (NNN) in a Cu host, as obtained within both the local-density approximation (LDA) and the generalized gradient approximation (GGA) for the exchange-correlation potential (V_{xc}). The experimental lattice constant of Cu is $a_{\text{exp.}} = 3.6149$ Å, while the theoretical values (a_{theory}) are 3.5228 and 3.6394 Å for LDA and GGA, respectively.

V_{xc}	LDA		GGA	
Lattice constant	a_{theory}	$a_{\text{expt.}}$	a_{theory}	$a_{\text{expt.}}$
NN to Bi	5.40%	6.07%	5.52%	5.33%
NNN to Bi	0.48%	0.61%	0.47%	0.44%
NN to Ir	1.44%	0.94%	0.97%	1.14%
NNN to Ir	0.20%	0.30%	0.27%	0.25%

this geometry were obtained as $\delta^s_{1/2} = 0.95$, $\delta^p_{1/2} = 1.39$, and $\delta^p_{3/2} = 0.89$.

In Table III we present the results for the skew-scattering contribution to the SHA of the Cu(Bi) alloy obtained from first-principles calculations. They are shown in comparison to Eq. (28) based on the spherical band approximation. The latter one provides good agreement with the Boltzmann equation. Including contributions of d and f electrons in Eqs. (23) and (13) results in almost the same value of 0.095. Thus, the assumption of Ref. 8, that the dominant scattering process in the Cu(Bi) alloy is related to p electrons, is confirmed. This is in agreement with Ref. 7, where it was highlighted that the spin-orbit driven scattering at Bi impurities is particularly high for p electrons. In addition, Table III demonstrates reasonable agreement between the results obtained by the Boltzmann equation and the Kubo-Středa formula. Taking into account the structural relaxation around the impurity leads to a reduction of the SHA by ∼20%, however this still cannot describe the experimental data.

Other options for an explanation of the discrepancy between theory and experiment are the intrinsic and side-jump mechanisms. For that reason we performed corresponding calculations for Cu(Bi) alloys with different impurity concentrations using the Kubo-Středa formula.[9] Figure 1 shows the results for the SHA including the intrinsic, side-jump, and skew-scattering contribution. The sign of this quantity remains positive for the whole range of the impurity concentrations analyzed in the experiment.[8] Altogether this demonstrates that the spin-orbit driven scattering at substitutional Bi impurities

TABLE III. The skew-scattering contribution to the spin Hall angle α for the dilute Cu(Bi) alloy calculated by means of the semiclassical and quantum-mechanical *ab initio* approaches as well as within the spherical band approximation. Here, the values in brackets are obtained including structural relaxation around the impurity atom.

Theory	SHA α
Phase-shift model, Eq. (28)	0.096 (0.089)
Boltzmann equation	0.081 (0.063)
Kubo-Středa formula	0.127
Experiment (Ref. 8)	−0.24

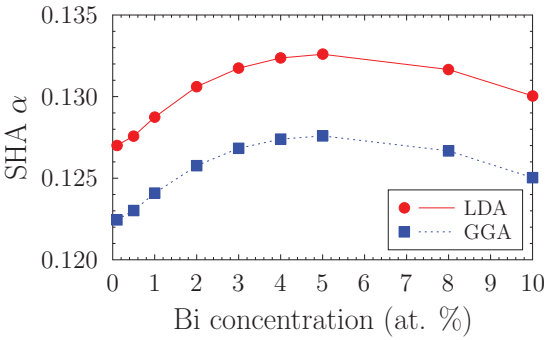

FIG. 1. (Color online) The spin Hall angle for the Cu(Bi) alloy with different impurity concentrations obtained from the Kubo-Středa formula using both the local-density approximation (LDA) and the generalized gradient approximation (GGA) for the exchange-correlation potential.

randomly distributed in bulk Cu cannot explain the sign of the measured SHA.

Thus, state-of-the-art *ab initio* calculations of the SHA cannot explain the existing experimental data for the Cu(Bi) alloy. However, the considered phase-shift model allows us to simulate the dependence of the SHA on the scattering properties by varying the corresponding phase shifts. Figure 2 shows α as a function of the phase shifts involved in Eq. (28). Here, we fix the difference between the two p phase shifts ($\delta^p_{1/2} - \delta^p_{3/2} = 0.50$) as obtained from our first-principles calculations for the relaxed geometry and vary $\delta^s_{1/2}$ and $\delta_p = \frac{1}{3}(\delta^p_{1/2} + 2\delta^p_{3/2})$. The SHA related to the *ab initio* phase shifts is situated in a stable positive region. However, certain combinations of the phase shifts can deliver the experimental result ($\alpha = -0.24$). As shown in the Supplemental Material,[29] a variation of the spin-orbit splitting $\delta^p_{1/2} - \delta^p_{3/2}$ which can be caused for instance by electron correlation effects, as proposed

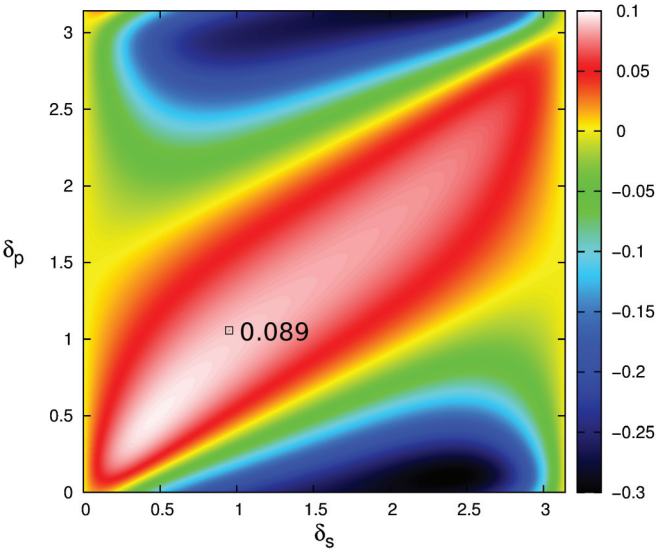

FIG. 2. (Color online) The dependence of the spin Hall angle, given by Eq. (28), on $\delta_s \equiv \delta^s_{1/2}$ and $\delta_p \equiv \frac{1}{3}(\delta^p_{1/2} + 2\delta^p_{3/2})$ is shown for the relaxed geometry together with the corresponding value of α from Table III.

in Ref. 30, would not change the sign of the SHA. Therefore, only a significant modification of the potential scattering properties could provide agreement between theory and experiment.

With respect to this finding, impurity cluster formation becomes increasingly important and is not considered in theory yet. Experimentally it was shown[8] that at impurity concentrations above 0.5 at. % Bi atoms start to segregate at the interface. For that reason the analysis to extract the skew-scattering contribution was restricted to lower concentrations. In this regime it was assumed that Bi impurities are randomly distributed without short-range ordering. This implies a linear relation between the impurity concentration and the resistivity of the studied films, which was observed for lower concentrations. However, the formation of extremely small clusters such as dimers or trimers down to lowest impurity concentrations could not be excluded and its impact on the SHE is, to date, not explored. For a description of that case the present theoretical approaches need to be extended. In addition, the existence of rough interfaces and grain boundaries in the films can cause extra scattering or can force the impurities to accumulate there, which would change the scattering properties as well. Indeed, recent studies[31–33] show such accumulations of Bi impurities at Cu grain boundaries.

VI. CONCLUSION

We performed a detailed analysis of the giant SHE in dilute Cu(Bi) alloys. Theory and experiment deliver a giant spin Hall angle but disagree with respect to sign. We demonstrated the agreement between different state-of-the-art *ab initio* calculations with respect to the skew-scattering contribution to the SHE from single Bi impurities in copper. The results of a generalized phase-shift model support the first-principles findings for both the magnitude and sign of the SHA, taking into account charge and lattice relaxation around the impurity. Furthermore, we have shown that the discrepancy can neither be explained by the side-jump contribution nor the intrinsic mechanism. Based on the generalized relativistic phase-shift model, we simulated the experimental data and found that only a strong modification of potential scattering can reproduce the measured SHA. This points to the existence of other scattering centers in the Cu(Bi) thin films than just randomly distributed substitutional Bi impurities. Possible candidates are few-atom clusters, interface roughness, and grain boundaries decorated with Bi atoms. Considerable changes of the scattering properties are expected for these cases in comparison to single substitutional Bi impurities. The corresponding verification by additional *ab inito* calculations and further experimental investigations is necessary.

ACKNOWLEDGMENTS

We are indebted to P. Levy, Y. Otani, and A. Fert for valuable discussions. The work was partially supported by the Deutsche Forschungsgemeinschaft (DFG) via SFB 762. The authors K.C., D.K., and H.E. acknowledge support from the DFG within SFB 689 and SPP 1538. In addition, M.G. acknowledges financial support from the DFG via a research fellowship (GR3838/1-1).

*dfedorov@mpi-halle.mpg.de

[1] M. I. Dyakonov and V. Perel, Phys. Lett. A **35**, 459 (1971).
[2] J. E. Hirsch, Phys. Rev. Lett. **83**, 1834 (1999).
[3] T. Seki, Y. Hasegawa, S. Mitani, S. Takahashi, H. Imamura, S. Maekawa, J. Nitta, and K. Takanashi, Nat. Mater. **7**, 125 (2008).
[4] L. Liu, C.-F. Pai, Y. Li, H. W. Tseng, D. C. Ralph, and R. A. Buhrman, Science **336**, 555 (2012).
[5] T. Tanaka, H. Kontani, M. Naito, T. Naito, D. S. Hirashima, K. Yamada, and J. Inoue, Phys. Rev. B **77**, 165117 (2008).
[6] M. Gradhand, D. V. Fedorov, P. Zahn, and I. Mertig, Phys. Rev. Lett. **104**, 186403 (2010).
[7] M. Gradhand, D. V. Fedorov, P. Zahn, and I. Mertig, Phys. Rev. B **81**, 245109 (2010).
[8] Y. Niimi, Y. Kawanishi, D. H. Wei, C. Deranlot, H. X. Yang, M. Chshiev, T. Valet, A. Fert, and Y. Otani, Phys. Rev. Lett. **109**, 156602 (2012).
[9] S. Lowitzer, M. Gradhand, D. Ködderitzsch, D. V. Fedorov, I. Mertig, and H. Ebert, Phys. Rev. Lett. **106**, 056601 (2011).
[10] A. Fert, A. Friederich, and A. Hamzic, J. Magn. Magn. Mater. **24**, 231 (1981).
[11] A. Fert and P. M. Levy, Phys. Rev. Lett. **106**, 157208 (2011).
[12] M. Gradhand, M. Czerner, D. V. Fedorov, P. Zahn, B. Y. Yavorsky, L. Szunyogh, and I. Mertig, Phys. Rev. B **80**, 224413 (2009).
[13] J. Sinova, D. Culcer, Q. Niu, N. A. Sinitsyn, T. Jungwirth, and A. H. MacDonald, Phys. Rev. Lett. **92**, 126603 (2004).
[14] G. Y. Guo, Y. Yao, and Q. Niu, Phys. Rev. Lett. **94**, 226601 (2005).
[15] Y. Yao and Z. Fang, Phys. Rev. Lett. **95**, 156601 (2005).
[16] G. Y. Guo, S. Murakami, T.-W. Chen, and N. Nagaosa, Phys. Rev. Lett. **100**, 096401 (2008).
[17] M. Gradhand, D. V. Fedorov, P. Zahn, I. Mertig, Y. Otani, Y. Niimi, L. Vila, and A. Fert, SPIN **2**, 1250010 (2012).
[18] Y. Niimi, M. Morota, D. H. Wei, C. Deranlot, M. Basletic, A. Hamzic, A. Fert, and Y. Otani, Phys. Rev. Lett. **106**, 126601 (2011).
[19] I. Mertig, Rep. Prog. Phys. **62**, 237 (1999).
[20] P. Strange, *Relativistic Quantum Mechanics* (Cambridge University Press, Cambridge, England, 1998).
[21] For simplicity, we skip the negligible small component in the corresponding Eq. (11.72) of Ref. 20, as was also used in Ref. 20 to obtain the scattering cross section given here by Eq. (14).
[22] E. Merzbacher, *Quantum Mechanics* (Wiley, New York, 1970).
[23] P. Monod and S. Schultz, J. Phys. (Paris) **43**, 393 (1982).
[24] D. A. Varshalovich, A. N. Moskalev, and V. K. Khersonskii, *Quantum Theory of Angular Momentum* (World Scientific, Singapore, 1988).
[25] W. Kohn and J. M. Luttinger, Phys. Rev. **108**, 590 (1957).
[26] According to Peter Levy (private communication), the derivation of Eq. (2) in Ref. 8 was based on the scattering-in term written as $\sum_{\mathbf{k}'} P_{\mathbf{k}'\leftarrow\mathbf{k}} g_{\mathbf{k}'}$, where $g_{\mathbf{k}}$ is the nonequilibrium part of the distribution

function. However, this differs from the correct scattering-in term derived by Kohn and Luttinger (Ref. 25) as $\sum_{\mathbf{k}'} P_{\mathbf{k}\leftarrow\mathbf{k}'} g_{\mathbf{k}'}$. In the nonrelativistic case the reversibility relation $P_{\mathbf{k}\leftarrow\mathbf{k}'} = P_{\mathbf{k}'\leftarrow\mathbf{k}}$ holds. However, the presence of the SOC leads to $P_{\mathbf{k}\leftarrow\mathbf{k}'} \neq P_{\mathbf{k}'\leftarrow\mathbf{k}}$ and $P^{\text{antisym}}_{\mathbf{k}'\leftarrow\mathbf{k}} = -P^{\text{antisym}}_{\mathbf{k}\leftarrow\mathbf{k}'}$, which causes opposite sign in the SHA evident from Eqs. (27) and (15).

[27] G. Kresse and J. Hafner, Phys. Rev. B **49**, 14251 (1994).

[28] P. E. Blöchl, Phys. Rev. B **50**, 17953 (1994).

[29] See Supplemental Material at http://link.aps.org/supplemental/10.1103/PhysRevB.88.085116 for the animation, which shows the change of Fig. 2 with an increase of the difference $\delta^p_{1/2} - \delta^p_{3/2}$ reflecting an enhancement of the SOC. Here, the corresponding values of the SHA from Table III for the unrelaxed and relaxed geometry are labeled by "+" and "□", respectively. One can see that the results of the phase-shift model remain stable with respect to the sign of the SHA for the full parameter space between 0 and π.

[30] B. Gu, I. Sugai, T. Ziman, G. Y. Guo, N. Nagaosa, T. Seki, K. Takanashi, and S. Maekawa, Phys. Rev. Lett. **105**, 216401 (2010).

[31] J. Luo, H. Cheng, K. M. Asl, C. J. Kiely, and M. P. Harmer, Science **333**, 1730 (2011).

[32] A. Kundu, K. M. Asl, J. Luo, and M. P. Harmer, Scr. Mater. **68**, 146 (2013).

[33] J. Kang, G. C. Glatzmaier, and S.-H. Wei, Phys. Rev. Lett. **111**, 055502 (2013).